Scientia Iranica A (2014) 21(3), 480–491

SCIENTIA IRANICA

Sharif University of Technology
Scientia Iranica
Transactions A: Civil Engineering
www.scientiairanica.com

Dynamic behavior of a tension leg platform offshore wind turbine under environmental loads

A. Ebrahimi[a,*], M. Abbaspour[b] and R. Mohammadi Nasiri[c]

a. *Faculty of Engineering and Applied Science, Memorial University of Newfoundland, St. John's, NL, Canada.*
b. *School of Mechanical Engineering, Sharif University of Technology, Tehran, Iran.*
c. *Department of Mathematical Science, Sharif University of Technology, Tehran, Iran.*

Received 26 July 2012; received in revised form 12 September 2013; accepted 28 October 2013

KEYWORDS
Offshore wind turbine;
Floating platform;
Tension leg platform;
Numerical solution;
Model test;
Sea wave load;
Wind load;
Fluid structure interaction.

Abstract. In order to evaluate the dynamic behavior of floating offshore wind turbines, the authors consider two approaches. A numerical method is used to investigate Tension Leg Platform (TLP) offshore wind turbine response behavior under a parked condition. This code considers nonlinearities due to changes in the tension of tethers. The off-diagonal components of stiffness, damping and mass matrices are considered to calculate coupling. This code solves the nonlinear equation of motion at each time step. However, in order to validate the data generated by the code, a scaled-down model was fully tested in the marine laboratory. The importance of these series of experiments is due to the fact that this model possesses a unique design and specifications to which no other model can be compared. Measurement of three degrees of freedom under environmental load is the goal of the experiments. Also, the results clearly show that the direction of encountering waves is an extremely important factor. It can be concluded that wind loads can dampen the oscillation of the model and prevent the impact of large loads on the tethers. The results show that the discrepancy between experimental and numerical results, with different degrees of freedom, is sufficiently acceptable.

1. Introduction

The shortage of energy from fossil fuel sources that we face in the coming years is a major motivation factor for policy makers to pay more attention to renewable energy sources, including offshore wind energy. The offshore field has been considered a promising resource for installing wind turbine farms. The development of technology in offshore wind turbines has resulted in the design and fabrication of 5 to 8 MW units. The relatively low surface roughness of the sea results in smoother and higher wind speeds. The offshore field also can remove other disadvantages of wind power, like noise pollution and undesired views. In shallow water below 50 m, wind turbines are mostly fixed to the sea bed. The cost of bottom mounted wind turbines is reasonably inexpensive. But, the use of bottom mounted wind turbines may not be feasible for deeper offshore locations. In addition to the limitation of water depth, wind farms should not interfere with any coastal transportation and the local tourism industry.

Some work has been carried out on this type of platform, such as oil platforms. Kibbee et al. [1-3], in much of their research work, examined the response behavior of the tension leg platform. Bhattacharyya et al. [4] investigated the coupled dynamics of mini TLP by developing a finite element code. Little work has been performed on floating platforms as offshore

*. *Corresponding author. Tel.: +98 851 2232346; Fax: +98 851 2221977*
E-mail addresses: Ae0046@mun.ca (A. Ebrahimi); Abbpor@sharif.edu (M. Abbaspour); Rmnasiri@gmail.com (R. Mohammadi Nasiri)

wind turbines. Wayman et al. [5] used the frequency domain to find Response Amplitude Operators (RAOs) for six degree of freedom to analyze various TLP and Barge designs. Withee [6] used an aero-servo-elastic design code, which was modified to include platform motion and hydrodynamic loading, based on Morisson's equation. Furthermore, some other work has been done on another type of platform, in particular, spar buoy offshore wind turbine platforms. Robertson and Jonkman [7] examined the load analysis of several offshore wind turbine concepts. Although the response of the spar buoy offshore wind turbine can be different, the methods used are similar to those used in this study. Karimirad et al. [8] analyzed the coupled dynamic motion of a catenary moored spar in harsh environments. Karimirad and Moan [9] examined the effect of waves and wind on the dynamic response of a catenary moored spar wind turbine.

The main purpose of this research is to demonstrate the dynamic behavior of a tension leg platform floating wind turbine. This research takes regular waves and wind load into account. Incorporating wind and waves has been used to produce the response amplitude operator of the model at three degrees of freedom: surge, heave and pitch. Also, in the experiments, the model has been tested at different angles between the direction of the waves and the forward leg in order to investigate the effects of these angles. The purpose of the second phase in the model testing (imposing wind load on the model), is not compared with the numerical model. It is just used to demonstrate the effect of wind damping on the model.

2. Numerical study

2.1. Feature of the model

There are many concepts which are designed to support a floating wind turbine. Three main models, which are more probable than others, are the pontoon, spar buoy and the tension leg platform. Urgent requirements for a floating support are:

- Support of its own weight and the weight of the turbine;
- Provision of an upright position and enough stability for all possible environments;
- Prevention of excessive and rough movement on the turbine;
- Satisfying economic constraints.

Every concept has its own advantages and disadvantages. The spar buoy is the simplest and easiest in design and fabrication. However, its catenary mooring lines are not stiff enough in different degrees of freedom. Since the smallest movement at the platform causes changes in the attack angle of the blades, it is imperative to maintain its efficiency, so that the wind turbine is not out of an upright position. The Pontoon concept needs a wide structure at the free surface to provide enough hydrostatic stiffness (GZ), but, this extensive structure at the free surface increases cost and wave load on the platform.

The three- and four-column tension leg platform has very good performance, and little movement in heave, pitch and roll. However, this concept is relatively complex and its cost is likely to be high.

A tension leg platform is a spar buoy which is stiffened by spokes and mooring lines under tension. So, it can combine the advantages of both the spar buoy and the tension leg platform. The wind turbine is attached to a vertical cylinder. The spokes and mooring lines are used to connect the cylinder to the anchors driven into the seafloor or gravity anchors. Pre-tension in the tethers allows the system to reduce pitch, roll and heave movements caused by winds and waves, but it still undergoes large surge motion. The stiffness which contributes to pitch, roll and heave is determined by the spring coefficient provided by the pre-tension in the lines and the length of the spokes. The amount of reserve buoyancy is a design parameter to keep the tethers in tension and causes excessive stiffness for the platform.

2.2. Theory

Assumptions:

The following assumptions were made in the analysis;

1. Initial pre-tension in all tethers is identical and is a constant value;
2. The linear wave theory was used to simulate wave surface elevation;
3. Wave forces are calculated at the instantaneous position of the platform by Morisson's equation;
4. Only a uni-directional wave is considered, so the model has three degrees of freedom.

2.2.1. Stiffness matrix

K_{ij} is the stiffness matrix coefficient of the model. The reactions in the degree of freedom, i, due to unit displacement in degree of freedom, j, were surge, heave and pitch, which are shown by Eqs. (1), (2) and (5). Due to cosine, sine, square, and square root terms, some components of the stiffness matrix are nonlinear. Figure 1 shows the upright position of the structure. The stiffness matrix is:

$$[K] = \begin{pmatrix} K_{11} & 0 & 0 \\ K_{31} & K_{33} & K_{35} \\ K_{51} & 0 & K_{55} \end{pmatrix}. \quad (1)$$

Surge components.

$$K_{11}x_1 = 8(T_0 + \Delta T_1)\sin\alpha_x, \quad (2)$$

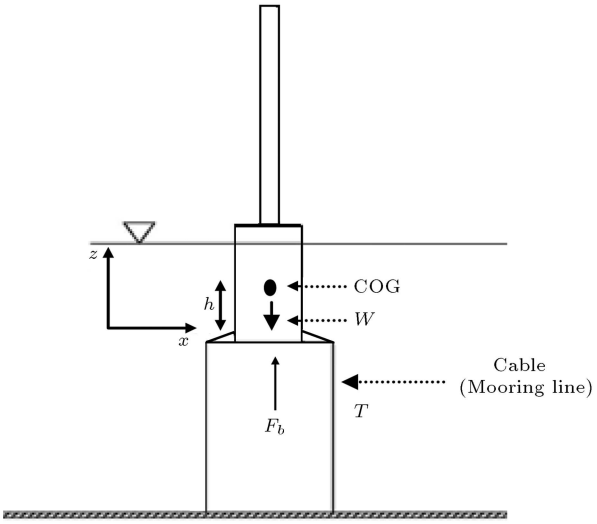

Figure 1. Schematic elevation of the tension leg platform offshore wind turbine.

where:

T_0	is the initial pre-tension in tethers;
ΔT_1	is change in initial pre-tension;
α_x	is the angle between initial position and instantaneous position at each time step.

We have:

$$\sin\alpha_x = \frac{x_1}{\sqrt{x_1^2 + L_1^2}}, \tag{3}$$

where:

x_1	is the displacement of the platform;
L_1	is the length of the mooring lines.

By substituting Eq. (3) in Eq. (2), we have:

$$K_{11} = 8\frac{(T_0 + \Delta T_1)}{\sqrt{x_1^2 + L_1^2}}. \tag{4}$$

Figure 2 shows the changes in mooring line positions due to the surge motion. Static equilibrium of forces in the direction results in:

$$K_{31}x_1 = 8T_0\cos\alpha_x + 8\Delta T_1\cos\alpha_x - 3T_0. \tag{5}$$

We have:

$$\cos\alpha_x = \frac{L}{\sqrt{x_1^2 + L_1^2}}. \tag{6}$$

Putting Eq. (6) in Eq. (5), we get:

$$K_{31} = \frac{(8T_0(\cos\alpha_x - 1) + 8\Delta T_1\cos\alpha_x)}{x_1}. \tag{7}$$

Static equilibrium of moments along pitch direction is:

$$K_{51}x_1 = -K_{11}x_1\bar{h}. \tag{8}$$

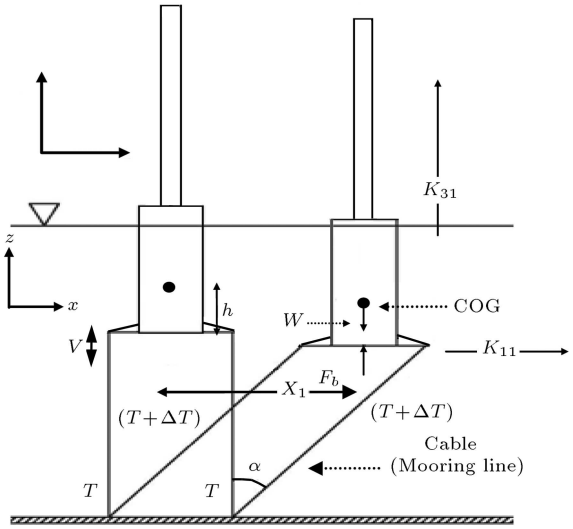

Figure 2. Displacement in surge degree of freedom.

By simplifying Eq. (8), we get:

$$K_{51} = -K_{11}\bar{h}, \tag{9}$$

where $\bar{h}$ is the distance between the Center of Gravity (CG) and the base of the cylinder. It is obvious that, as the force K_{11} acts at the bottom of the cylinder, it exerts the moment along the pitch direction on the model.

Heave components. Since no forces arise in the surge direction due to arbitrary displacement in the heave direction, $K_{13} = 0$.

The static equilibrium of forces in the heave direction gives:

$$K_{33} = \frac{8A_cE}{L} + \rho g A_c d, \tag{10}$$

where:

E	is the elasticity of tethers;
d	is the draft of the cylinder;
g	is the acceleration of gravity;
A_c	is the area of the cylinder;
ρ	is the mass density of water.

Since no moment arises along the pitch direction due to arbitrary displacement along the heave direction, $K_{53} = 0$.

Pitch components. Since no force arises in the surge direction due to arbitrary displacement along the pitch direction, $K_{15} = 0$. By exerting an arbitrary rotation, θ_5, along the pitch direction, pre-tension in the tethers changes, which is equal to:

$$\Delta T_5 = \frac{A_tE}{L}\left(\left(\frac{D}{2} + L_{\text{spoke}}\right).\cos\theta_5\right)\theta_5, \tag{11}$$

where ΔT is change in the initial pre-tension of the

tethers due to arbitrary rotation along the pitch direction. Since, in the z direction, pre-tension in half of the mooring lines increases by ΔT and in others it decreases by ΔT, there is no force in the heave direction. So, $K_{35} = 0$.

Buoyancy force in the cylinder is equal to:

$$F_b = \rho g A_c d. \tag{12}$$

The static equilibrium of moment along the pitch direction is:

$$K_{55} = F_b(GZ) + 2(T_0 + \Delta T_5)P_a, \tag{13}$$

where:

$$P_a = \frac{D}{2} + L_{\text{spoke}}. \tag{14}$$

GZ is the height of the metacenter, which is an important parameter in the stability of any floating structure. Figure 3 shows the changes in the mooring line position due to the pitch motion.

2.2.2. Mass matrix

Since the natural mass of the system does not change, initial values of mass matrix components are constant and diagonal.

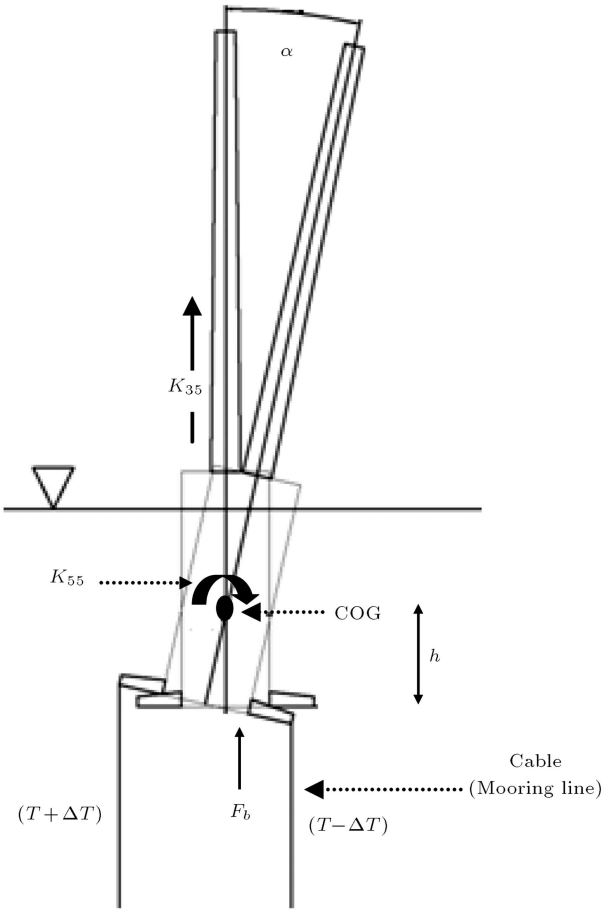

Figure 3. Displacement in pitch degree of freedom.

But when the system possesses motion and acceleration, it accelerates the surrounding water causing added mass. So when the system fluctuates, not only do its diagonal components change, but also its off-diagonal components change.

$$[M] = \begin{pmatrix} M_{11} + M_{a11} & 0 & M_{a15} \\ 0 & M_{33} + M_{a33} & 0 \\ M_{a51} & 0 & M_{55} + M_{a55} \end{pmatrix}$$

$$M_{11} = M_{33} = M, \tag{15}$$

M is the mass of the structure, and M_{55} is the mass moment of inertia about the y-axis.The added mass can be calculated by the method used by Withee [10]:

$$M_{a11} = A_c[c_m - 1]\rho.d.\ddot{x}_{\text{surge}}, \tag{16}$$

$$M_{a33} = A_c[c_m - 1]\rho.d.\ddot{x}_{\text{heave}}, \tag{17}$$

$$M_{a51} = \frac{1}{8}.\rho.\pi.D^2.\ddot{\theta}_5.d, \tag{18}$$

$$M_{a15} = \frac{1}{8}.\rho.\pi.D^2.\ddot{x}.d^2, \tag{19}$$

$$M_{a55} = \frac{1}{12}.\rho.\pi.D^2.\ddot{\theta}_5.d^3. \tag{20}$$

M_{a51} is the added mass moment of inertia along the pitch direction due to the hydrodynamic force in the surge direction; and M_{a15} is the added mass moment of inertia along the surge direction due to the hydrodynamic force in the pitch direction. In most work, $C_m = 2$ is considered.

2.2.3. Damping matrix

Based on the Rayleigh method in structural dynamics, the damping matrix is assumed to be proportional to stiffness and mass matrix. But, for $[K]$ and $[M]$, the initial values of the diagonal components must be used. $[C]$ is calculated by:

$$[C] = \alpha[M] + \beta[K]. \tag{21}$$

α and β are constant values.

2.2.4. Hydrodynamic forces

The problem of a suitable theory to simulate the wave environment is a prime concern here. Once the suitable theory is considered to evaluate the wave environment, the wave loading on the model can be calculated with enough accuracy. According to the Caspian Sea topography and the Wilson method [10], the airy wave theory is suitable for computing the water particle position, η:

$$\eta = A\frac{\cosh(K.(d+\eta))}{\sinh(K.h)}\cos(K.x - \omega.t), \tag{22}$$

where A is the amplitude of the waves, K is the wave number, ω is the wave frequency and x is the horizontal distance from the origin. The fluctuating free surface can be a significant part of hydrodynamic loading when wave amplitude cannot be ignored in comparison to water depth.

According to Chakrabarti [11], the following equation for horizontal water particle velocity is suggested, which incorporates the effects of variable submergence:

$$u = A.\omega.\cos(K.x - \omega.t).\frac{\cosh(K.(d+\eta))}{\sinh(K.h)}. \tag{23}$$

Likewise, the horizontal water particle acceleration equation and, also, its vertical water particle equations, get modified.

$$\dot{u} = A.\omega^2.\sin(K.x - \omega.t).\frac{\cosh(K.(d+\eta))}{\sinh(K.h)}, \tag{24}$$

$$w = A.\omega.\sin(K.x - \omega.t).\frac{\sinh(K.(d+\eta))}{\sinh(K.h)}, \tag{25}$$

$$\dot{w} = -A.\omega^2.\cos(K.x - \omega.t).\frac{\sinh(K.(d+\eta))}{\sinh(K.h)}. \tag{26}$$

As a structure frequently has displacements in various degrees of freedom, relative velocity and acceleration must be taken into account. α_z and α_x are the angle of the cylinder axis to the vertical, and angle of the cylinder projection to the x-axis.

$$\{C\}^T = \{C_x, C_z\}, \tag{27}$$

$$C_x = \sin\alpha_z.\cos\alpha_x, \tag{28}$$

$$C_z = \cos\alpha_z. \tag{29}$$

The velocities and accelerations should be modified by these factors:

$$u_x = u - C_x(C_x.u + C_z.w), \tag{30}$$

$$\dot{u}_x = \dot{u} - C_x(C_x.\dot{u} + C_z\dot{w}), \tag{31}$$

$$u_z = w - C_z(C_x.u + C_z.w), \tag{32}$$

$$\dot{u}_z = \dot{w} - C_z(C_x.\dot{u} + C_z\dot{w}). \tag{33}$$

Since the diameter of the cylinder is negligible in comparison to the significant wave length of the Caspian Sea, the hydrodynamic forces exerted on the cylinder could be calculated just by Morisson's equation.

$$|\{U_N\}| = \sqrt{u_x^2 + u_z^2}, \tag{34}$$

$$f_x = c_m.\rho.\frac{\pi.D^2}{4}.\ddot{u}_x + c_d.\frac{\rho}{2}.D.|\{U_N\}|.(\dot{u}_x - \dot{x}) \pm \frac{\pi.D^2}{4}.(c_m - 1).\rho.\ddot{x}, \tag{35}$$

$$f_z = c_m.\rho.\frac{\pi.D^2}{4}.\ddot{u}_z + c_d.\frac{\rho}{2}.D.|\{U_N\}|.(\dot{u}_z - \dot{z}) \pm \frac{\pi.D^2}{4}.(c_m - 1).\rho.\ddot{z}, \tag{36}$$

f_x and f_z are the forces per unit length of the structure. A summation of all elements should be taken to present total forces. The last term in each of the equations is added to the mass term, and a positive sign is used when the water surface is below the MSL. When the water surface is above the MSL, a negative sign should be used. Wilson [10], by means of the dimension of a cylinder and the characteristics of encountered waves, presents constant values for c_m and c_d.

F_x and F_z are the total forces which cause displacements in x and z directions. Also, M_y is the moment of inertia causing rotation along the direction. The force matrix is:

$$F_x = \int_c f_x.dz + \int_s f_x.dz, \tag{37}$$

$$F_z = \int_c f_z.dx + \int_s f_z.dx, \tag{38}$$

$$M_y = \int_c (f_x \times z).dz + \int_s (f_x \times z).dz + \int_c (f_z \times x).dx + \int_s (f_z \times x).dx. \tag{39}$$

$\{F(t)\}$ is the force vector, where:

$$\{F(t)\} = \{F_x, F_z, M_y\}^T. \tag{40}$$

2.2.5. Aerodynamic

The wind speed measured in the field shows variations in time, direction and speed. Actual wind speed is characterized by two important features: Turbulence and wind shear.

Wind shear. The wind speed is affected by the friction surface in the lower 2 km of the Earth's atmosphere. The Earth's boundary layer reduces wind speed from its undisturbed value at 2 km height to nearly zero at the surface. To describe this boundary layer effect, two models are used by Temple et al. [12]; the logarithmic profile and the power law profile. Both models can be used with enough accuracy. The

logarithmic and power law profiles are described by Eqs. (41) and (42), respectively:

$$V_w(z) = V_{w,r}.\frac{\ln(z/z_0)}{\ln(z_r/z_0)}, \tag{41}$$

with:

$V_w(z)$	mean wind speed at height z;
$V_{w,r}$	mean wind speed at the reference height z_r;
z_r	reference height;
z_0	surface roughness-length.

Det Norske Veritas (DNV) and Germanischer Lloyd (GL) advise in their offshore regulations to use $z_0 = 0.05$ and $z_0 = 0.002$, respectively. In this paper, the logarithmic method is used, and $z_0 = 0.05$ is considered in calculations.

Turbulence. When wind is measured in a field, a time varying wind speed can be found. Two statistical parameters can be calculated on a time series: The mean wind speed and the standard deviation. The turbulence intensity is defined as the standard deviation of the time varying wind speed divided by the mean wind speed, which is usually presented as percentages:

$$I_t = (\sigma/V_w). \tag{42}$$

The roughness of the terrain is the most important factor to determine the turbulence intensity. There are different standards that describe the turbulence intensity as a function of wind speed for various terrains. Germanischer Lloyd (GL) offers $I_t = 12\%$ for $V_w = 23$ m/s, an offshore field. Figure 4 illustrates a 1-hour turbulent wind in comparison to a 1-hour mean wind.

Loads. To calculate the wind load on the tower, an equation similar to the Morisson's equation can be used. The wind load on the tower section is given by:

$$F_{\text{aero}} = \frac{1}{2}C_{\text{aero}}.p_{\text{air}}.A.V^2_{\text{section}}, \tag{43}$$

with:

F_{aero}	wind load;
C_{aero}	aerodynamic coefficient (shape, surface dependent);
p_{air}	density of air;
A	exposed area of the section;
V_{section}	wind velocity at the center of the section.

2.2.6. Equation of motion

The dynamics of every structure in the presence of damping, mass, stiffness and force terms is described by the general equation of motion:

$$[M]\{\ddot{X}\} + [C]\{\dot{X}\} + [K]\{X\} = \{F(t)\}, \tag{44}$$

where:

$\{\ddot{X}\}$	is the acceleration vector of the structure;
$\{\dot{X}\}$	is the velocity vector of the structure;
$\{X\}$	is the displacement vector of the structure;
$[C]$	is the damping matrix;
$[K]$	is the stiffness matrix;
$[M]$	is the mass matrix, and;
$[F]$	is the load vector.

Formulations for the calculation of $[C]$, $[K]$, $[M]$ and $[F]$ have already been explained in detail. The force vector, fluctuation in added mass, stiffness and, consequently, damping matrix, depend on the response of the structure in the previous step. So, the procedure of solving becomes iterative. Because of the instability of the system in the solving procedure, the first 100 seconds of all plots of displacement, velocity and acceleration have been neglected. This equation was solved by the ode45 method.

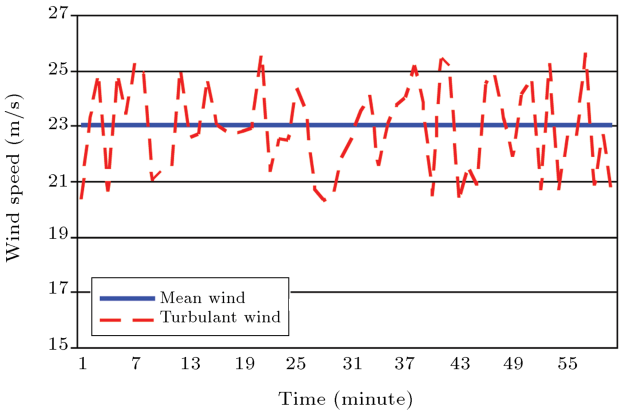

Figure 4. Time history of turbulent 1-hour wind and mean 1-hour wind.

2.3. Load conditions

In order to examine the model under various environmental conditions, three load cases are considered. In load conditions 1 and 2, two different wave heights are imposed on the model, but, without the contribution of wind load, in order to show the relationship between the wave height and the responses of the model. Hydrodynamic conditions of load case 3 are like load case 2, but, in case 3, wind loads are taken into account in the form of shear and turbulent flow. The purpose of this case is to demonstrate wind effects on the model under similar hydrodynamic conditions. Table 1 shows the load cases.

Table 1. Environmental conditions.

Load case	Wind conditions	Wave conditions
1	None: air density= 0	Regular wave: $H_s = 3.3$ m, $T_s = 9.5$ s[a]
2	None: air density= 0	Regular wave: $H_s = 6.6$ m, $T_s = 9.5$ s
3	Turbulent, shear, V_h[b]	Regular wave: $H_s = 6.6$ m, $T_s = 9.5$ s

[a]: T_s: significant wave period; H_s: significant wave height.

[b]: V_h: 1-hour wind speed.

Table 2. Static specifications of the three considered concepts.

Static properties	Model 1	Model 2	Model 3
Platform diameter	18 (m)	34 (m)	29 (m)
Draft	47.89 (m)	10.79 (m)	21.73 (m)
Mooring system angle	90 (deg)	90 (deg)	90 (deg)
Number of mooring lines	8	8	8
Total displacement	12181 (tons)	9800 (tons)	14350
Platform mass	8600 (tons)	8000 (tons)	8300 (tons)
Length of spokes	9 (m)	9 (m)	9 (m)

Table 3. The 5-MW turbine specifications.

Wind turbine properties	Values
Rated power	5 (MW)
Rotor diameter	126 (m)
Hub height	90 (m)
Nacelle mass	240 (tons)
Tower mass	347 (tons)
Rotor mass	110 (tons)
Center of mass location	64 (m)

2.4. The models

For this paper, three models by Slavounos et al. [13], which are assumed as probable concepts for a tension leg platform offshore wind turbine, are considered. The specifications of all models and the wind turbine used for all models are shown in Tables 2 and 3.

2.5. Results and discussions

The model oscillates with imposed wave length. The results show that the most considerable motion, in comparison with other types of motion, is surge. But, an advantage of the TLP platforms is that tensioned mooring lines do not let the model oscillate with large pitch. If the platform of an offshore wind turbine possesses large pitch, it brings about less efficiency because of changes in the turbine blade pitch angle. In addition, it exerts more acceleration on the tower, so, it fails sooner because of fatigue.

By comparing Table 4 with Table 5, it can be seen that when wave height becomes 2-times larger, the response of the system is more than two times larger.

Table 4. Responses of the three models under load case 1.

Model	Surge (m)	Heave (m)	Pitch (rad)	Maximum horizontal acceleration (m/s^2)
#1	1.17	0.01	-0.005	0.039
#2	0.78	0.18	-0.017	0.018
#3	0.90	0.07	-0.009	0.035

Table 5. Responses of the three models under load case 2.

Model	Surge (m)	Heave (m)	Pitch (rad)	Maximum horizontal acceleration (m/s^2)
#1	3.20	0.11	-0.016	0.65
#2	2.40	0.81	-0.069	0.41
#3	2.90	0.36	-0.029	0.59

This is because Morisson's equation is according to the square of water velocity relative to structure velocity in its inertia term.

All results in Tables 4 and 5 indicate that model 1 has less movement in the heave and pitch, and this is not just because of its larger moment of inertia. According to Eq. (22), as the depth of water increases, the movement and velocity of the water particles decrease. It means that maximum movements, velocities and acceleration of water particles are at the free surface and are nearly zero at the bottom. Consequently, as the draft of the platform increases, less vertical loads

Table 6. Responses of the three models under load case 3.

Model	Surge (m)	Heave (m)	Pitch (rad)	Maximum horizontal acceleration (m/s^2)
#1	3.04	0.11	-0.015	0.60
#2	2.30	0.81	-0.064	0.39
#3	2.82	0.36	-0.025	0.56

are imposed on the bottom of the platform, resulting in less movement in the heave and pitch.

In Table 6, the effects of the wind loads are demonstrated. As wind loads exert pressure on the tower, the model has to use part of its energy to overcome this pressure. So, wind loads can be assumed significant damping factors. Wind loads can make larger offsets for the surge and pitch, but, actually, decrease the ranges of oscillation and acceleration insignificantly.

3. Experimental study

3.1. Similitude criterion

Modeling and scaling down the prototype to test in a marine laboratory is a common practice, and the modeling criterion and laws are presented well in Chakrabarti [11]. The principle of dynamic modeling is to scale down the forces dominating the full scale. Any two forces in a prototype condition should be scaled with respect to the ratio between the prototype and the model. As strict adherence to the laws of scaling is actually impossible, those forces that primarily affect the phenomena should be taken into account. In this study, the Froude number law was considered to be a prominent law used to scale the floating structure test conditions. Froude's law justifies the relation between inertia forces and the weight of the fluid particles. In a free surface, the water gravity force is significant, so, gravitational forces should be balanced by inertia forces. Froude is used to demonstrate the ratio between these two forces. The Froude number is defined as:

$$F_r = \frac{u^2}{gL}, \tag{45}$$

where u, g and L are the fluid velocity, gravitational acceleration and characteristic dimension of the structure, respectively. Since the Froude number is a non-dimensional number, it can satisfy this equation:

$$\frac{u_p^2}{gL_p} = \frac{u_m^2}{gL_m}, \tag{46}$$

where p and m identify the prototype and model, respectively. If λ is assumed to be the ratio between the characteristic dimensions of the prototype and the model, from Eq. (2), we have:

$$u_p = \sqrt{\lambda}.u_m. \tag{47}$$

Other important parameters can be derived as:

$$m_p = \lambda^3.m_m, \tag{48}$$

$$F_p = \lambda^3.(\rho_p/\rho_m).F_m, \tag{49}$$

$$\dot{u}_p = \dot{u}_m, \tag{50}$$

$$t_p = \sqrt{\lambda}.t_m, \tag{51}$$

where m, F, $\dot{u}$ and t are mass, force, fluid acceleration and time, respectively. In the modeling of offshore structures, since the tethers are significant in the stiffness of the structure, the characteristics of tethers should also be scaled down. These significant parameters are elasticity, diameter and mass per unit length of the tether.

Since the stiffness is scaled with λ^2, this equation can be resulted:

$$\frac{(A.E/L)_p}{(A.E/L)_m} = \lambda^2, \tag{52}$$

where E is the elasticity of the tethers, A is the cross-section area and L is the length of tethers.

Because of existing limitations in the laboratory, such as depth of flume, a model which is 1/135 the scale of a 5-MW tension leg platform offshore wind turbine, was built for the experimental study. All specifications of the scaling procedure are presented in Table 7.

The blades and hub were not fabricated, but, the specifications of the turbine, such as center of gravity, mass and moment of inertia, which have great effects on the responses of the model, were considered. The specifications of a 5-MW wind turbine used in previous works, like Matha [14], are shown in Table 8.

3.2. Experimental set-up

The set-up was held in a flume, 3 m wide, 25 m long and 1.1 m deep. The flume is equipped by a flapping wave maker to generate regular waves. In order to prevent the reflection of the generated waves, an artificial beach, 2 m long and with a 30 degree slope, was installed at the end of the flume. In-place calibrations were accomplished precisely for a load cell, which was used to measure induced tension in the tethers of the model. Figure 5 shows the model in an upright position with its tension sensors. Also, two cameras were installed at two different positions to record the displacements of the model and waves during the experiments, which were to be used for image processing. Some conditions which should be considered for image processing, such as different colors

Table 7. Specifications of the model and 5-MW prototype.

Parameter	5-MW	Model
Displacement	12187000 (kg)	4.95 (kg)
Weight	8600000 (kg)	3.80 (kg)
Average mooring system tension per line	3543 (kN)	1.47 (kN)
Average mooring system tension per leg	7086 (kN)	2.94 (kN)
Water depth	150 (m)	1.1 (m)
Draft	47.89 (m)	35 (cm)
Diameter of the cylinder	18 (m)	13 (cm)
Length of the a pontoon	18 (m)	13 (cm)
Vertical center of gravity	−32.76 (m)	−24 (cm)
Number of the tethers	8	8
Length of the tethers	102.11 (m)	75 (cm)
Stiffness of the tethers	1500000 (kN)	11111 (kN)

Table 8. The 5-MW turbine specifications.

Wind turbine properties	Values
Rated power	5 (MW)
Rotor diameter	126 (m)
Hub height	90 (m)
Nacelle mass	240000 (kg)
Tower mass	347460 (kg)
Rotor mass	110000 (kg)
Center of mass location	64 (m)

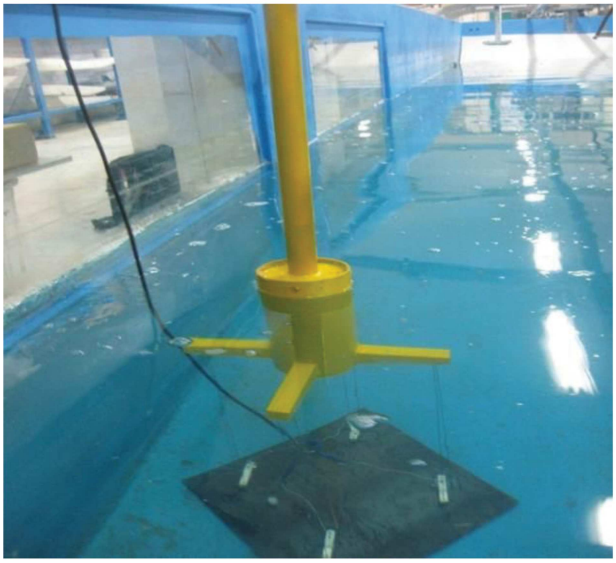

Figure 5. The model and measuring apparatus which are ready to run.

for the model and its background, and the perpendicularity of the cameras with respect to the model and waves, were done. Computer software was used to translate the films recorded during the experiments. A load cell and data logger can take 50 samples per second, and this rate of sample taking improves the accuracy of measurements. A wind generator was used which can generate wind at various speeds and with a maximum speed of 12 m/s, in order to demonstrate the wind effects on the tower of the model. This wind generator is equipped with 4 m long tunnel to make the wind velocity laminar. Figure 6 shows the model under wind and wave loading. In order to have a better understanding of the model and its set-up, the model is shown in Figure 7.

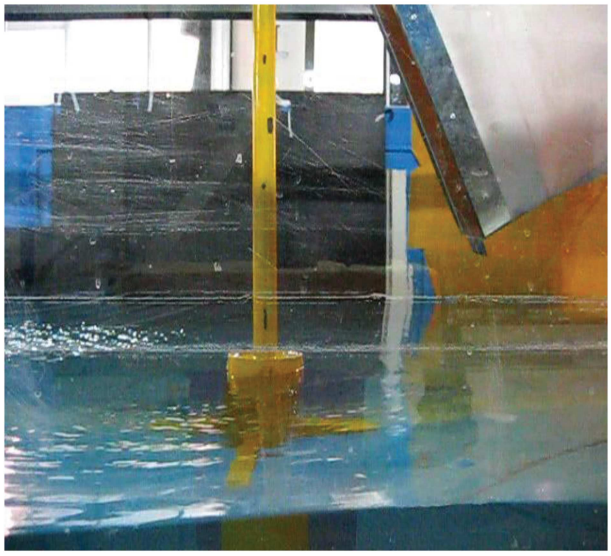

Figure 6. The model under effect of wind and waves loads.

3.3. Load cases

The experiments should be mainly divided into two different load cases: 1) The model is under only hydrodynamic loads, 2) The model is under hydrodynamic and aerodynamic loads.

The goals of the first phase are to demonstrate the natural frequency of the model by means of Response

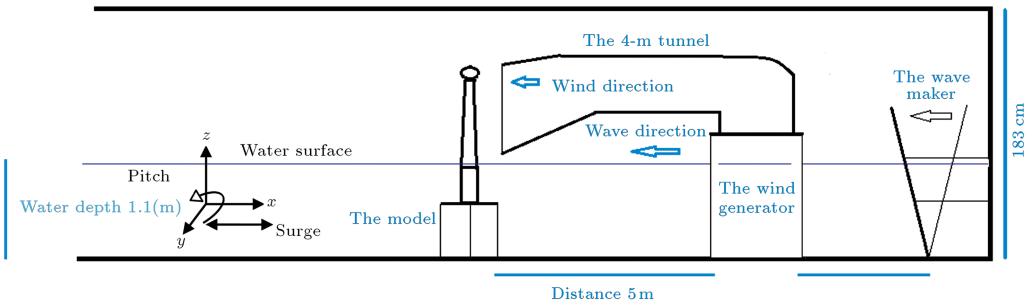

Figure 7. Sketch of the set-up illustrating the wave flume, the wind generator and the wind turbine.

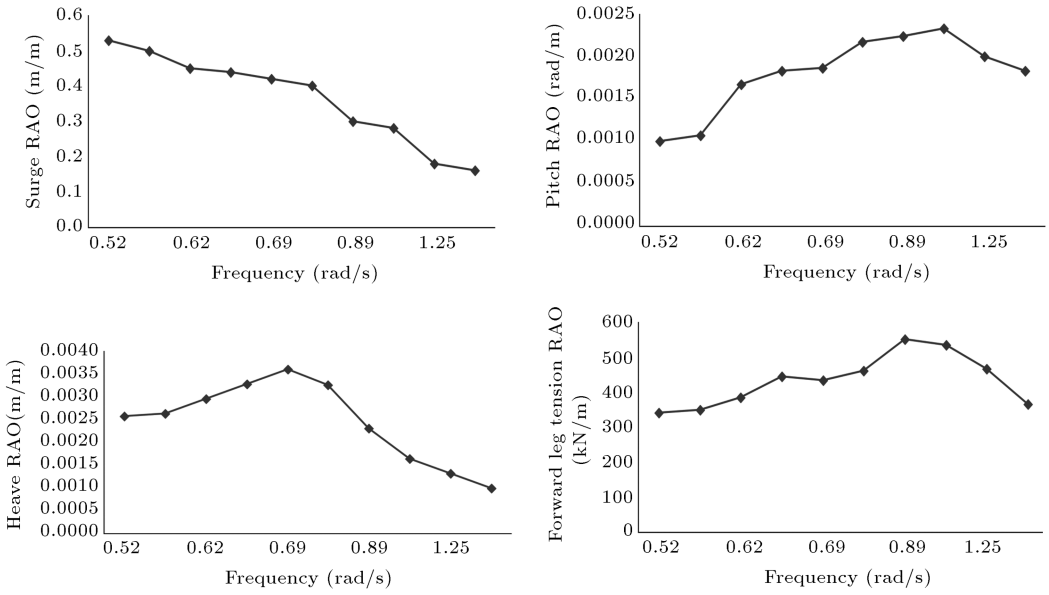

Figure 8. The 5-MW wind turbine RAOs against load case 1.

Amplitude Operators (RAOs) graphs. A series of waves in the range of 0.3 to 3 m wave lengths, and 3 cm in height, were exerted to produce RAO graphs, and 10 years of significant waves, with 2.6 m wave lengths and 9 cm in height, to test the model under the significant wave conditions of the Caspian Sea.

Because of the fact that the shape of the model is not axis-symmetric, both the inertia and drag terms of the Morrison equation change at different encountering wave angles. Consequently, the angle between the forward leg and the propagating waves is so important in the dynamic response behavior of the model, that the model was put into various angles: 0, 30, 45 and 60 degrees.

The purpose of phase two is to demonstrate the effects of wind loads on the tower, and the dynamic response behavior of the model. So, in addition to that series of waves used to produce RAOs, the model was tested at two different wind speeds: 6 and 12 m/s. These speeds are measured at the hub position, and the wind is in the shape of shear flow. The wind was made laminar to produce a maximum drag on the cylinder shaped tower.

3.4. Results and discussions

By studying Figure 8, as the significant wave frequency of the determined area of the Caspian Sea for installing the offshore wind turbine is 0.66 rad/s, it can be inferred that the prototype can evade the natural frequency of pitch and induced tension in the tethers. Contrary to surge, the pitch brings about impacts on the mooring lines. This is an important design criteria for TLP platforms to prevent extra tension on the mooring lines.

It is expected that the angle between encountering waves and the forward leg cannot be effective in the response behavior of the platform, since the principle part of the model is a cylinder, whose shape is axis-symmetric and whose legs are located so far from the free surface that water particles possess more motion. On the contrary, the experiments performed show that, as much the angle between the forward leg and encountering waves becomes larger, the surge response becomes larger too. This is evident in Figure 9 and Table 9.

Imposed wind on the tower can affect the dynamic response behavior of the structure. Because of this,

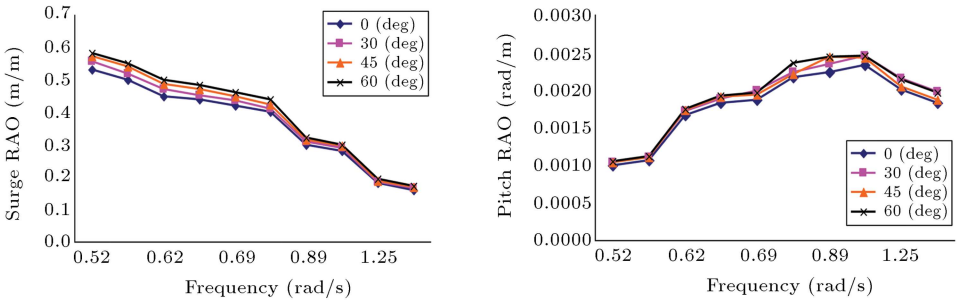

Figure 9. Surge and pitch RAOs comparison for different angles against load case 1.

Table 9. Effects of angles between encountering waves and forward leg in surge response.

Sea states	H (m)	3	6.6
	T (s)	9.5	9.5
Surge (m)	0 (deg)	1.70	3.90
	30 (deg)	1.90	4.10
	45 (deg)	2.00	4.25
	60 (deg)	2.10	4.30

there are several damping factors which can affect the behavior of the structure: hydrodynamic drag damping, vortex damping, and aerodynamic drag damping. When a structure has to use some amount of energy to overcome aerodynamic drag, the imposed wind dampens the range of the displacements, especially the surge and pitch. Although wind itself has an initial displacement on the structure, it decreases the amplitude of the oscillations. This is significant in two aspects: First, an offshore wind turbine should possess soft and low movements, so that the turbine can operate well and at maximum efficiency. Second, the most risky components of the tension leg platform are the tethers, which are under high tension. Large and sharp movements induce heavy loads on the tethers of the structure. Lastly, it can be concluded that wind prevents extra tension in the tethers.

Wind loads are assumed to be an important matter in offshore wind turbines. The performed experiments show that only wind can make a larger offset for the model, but, when hydrodynamic loads (waves) are exerted, the wind loads on the tower nearly lose their effectiveness. That is probably because of the density of water, which results in much more load in comparison to the wind, and this high density of water allows the waves to control the dynamic behavior of the wind turbine. When the height of the waves is low, the wind loads on the tower play their own role, partially in the behavior of the model. It must be mentioned that H and T are given at full scale, but the wind speed is reported at model scale. Table 10 describes the effects of wind loads on the tower.

Table 10. Effects of wind loads on the tower of 5-MW wind turbine.

Sea states	H (m)	3	6.6
	T (s)	9.5	9.5
Surge (m)	0 (m/s)	1.70	3.90
	6 (m/s)	1.70	3.90
	12 (m/s)	1.60	3.80

3.5. Summary and conclusions

In this study, a numerical method is used to investigate the 5-MW tension leg platform offshore wind turbine response behavior under parked conditions. This code takes the off-diagonal components of stiffness, damping and mass matrices into account, in order to evaluate the coupling of surge and pitch. Also, this code considers nonlinearities due to changes in the tension of tethers, so, it can present the results of the model motion with enough accuracy. Furthermore, shear turbulent wind is exerted on the tower, with maximum speed of 30 m/s on the hub. This research considers various environmental conditions to demonstrate the effects of waves and wind, individually, on the models. Also, three models are tested to find the best performance of these models under determined environmental conditions. In order to validate data generated by the code, an experimental study was accomplished on the 1/135 scaled down model of the 5-MW tension leg platform offshore wind turbine at the Sharif University of Technology Marine Laboratory in order to investigate the dynamic response behavior of the model. The response time series of the 3 degrees of freedom: surge, heave, pitch, and forces induced in the forward leg, were measured. In addition, the model was tested at various angles between encountering waves and the forward leg. The results of the model have been scaled up by appropriate scale factors.

The results show that the most considerable motion, in comparison to other motion, is surge, but, tension induced in the tethers nearly is proportional to pitch motion. The results clearly show that the direction of encountering waves is an extremely important factor in the response behavior of the model. Also, it can be concluded that wind loads on the tower

can be effective when the height of the waves is small. Wind loads on the tower can dampen the oscillation of the model and prevent inducing large loads on the tethers. By going through the results of the analyses, it is obvious that discrepancies between results in surge, heave and pitch movements are 13%, 8% and 10%, respectively. Therefore, it can be concluded that although there are differences between the results of the numerical and experimental methods, it is still a suitable method for calculating the movements of this model, because these discrepancies are acceptable and negligible. These differences are caused by nonlinearity in the waves, the effect of diffraction, and tethers that sometimes possess unpredictable shapes appearing in experiments. Because of the fact that surge motion includes more nonlinearity factors, discrepancies between the results of numerical and experimental approaches is more comparable to heave and pitch motions.

Acknowledgments

The authors wish to thank Professor Mohammad Saeid Seif and the staff of Sharif University Marine Laboratory for their help at different stages of this research.

References

1. Kibbee, S., Chianis, J., Davis, K.B. and Sarwono, B.A. "The tension leg platform", *Offshore Technology Conference, OTC 7535*, pp. 243-256 (1994).
2. Kibbee, S., Chianis, J., Davis, K.B. and Sarwono, B.A. "A miniplatform for deep water - the TLP", *Society of Naval Architects and Marine Engineer Conference* (1995).
3. Kibbee, S., Leverette, S.J., Davis, K.B. and Matten, R.B. "Morepeth mini-TLP", *Offshore Technology Conference.* OTC10855 (1999).
4. Bhattacharyya, S.K., Sreekumar, S. and Idichandy, V.G. "Coupled dynamics of tension leg platform", *Ocean Engineering*, **30**, pp.709-737 (2003).
5. Wayman, E.N., Sclavounos, P.D., Butterfield, S., Jonkman, J. and Musial, W. "Coupled dynamic modeling of floating wind turbine system", *Proceedings: The Offshore Technology Conference*, Houston, Texas (2006).
6. Withee, J. "Fully coupled dynamic analysis of a floating wind turbine system", PhD Dissertation, Massachusetts Inst. of Tech (2004).
7. Robertson, A.N. and Jonkman, J.M. "Loads analysis of several offshore floating wind turbine concepts", in *Proceedings the of 21st International Offshore and Polar Engineering Conference*, Maui, Hawaii, USA, pp. 443-450 (2011).
8. Karimirad, M., Gao, Z. and Moan, T. "Dynamic motion analysis of catenary moored spar wind turbine in extreme environmental condition", *Offshore Wind Conference*, Sweden (2009).
9. Karimirad, M. and Moan, T. "Wave and wind induced dynamic response of catenary moored spar wind turbine", *Journal of Waterway, Port, Coastal, and Ocean Engineering*, **138**(1), pp. 9-20 (2012).
10. Wilson, J.F., *Dynamics of Offshore Structure*, John Wiley & Sons, New jersey, USA, pp. 61-75 (2003).
11. Chakrabarti, S.K., *Offshore Structure Modeling*, World Scientific, Singapore, pp. 123-124 (1994).
12. Temple, J.D., Twidell, J. and Gaudiosi, G., *Offshore Wind Power*, Multi-Science, England, pp. 162-164 (2009).
13. Slavounos, P., Tracy, C. and Lee, L. "Floating offshore wind turbines: Responses in a seastate Pareto optimal designs and economic assessment", *International Conference on Offshore Mechanics and Arctic Engineering*, San Diego, pp. 31-41 (2007).
14. Matha, D. "Model development and loads analysis of an offshore wind turbine on a tension leg platform with a comparison to other floating turbine concepts", Report NREL/SR-500-45891 (2009).

Biographies

Alireza Ebrahimi obtained a BS degree from Amirkabir University of Technology, Tehran, Iran, in Naval Architecture and Marine Engineering in 2009, and an MS degree from the School of Mechanical Engineering of Sharif University of Technology, Tehran, Iran, in 2011. He then entered the Memorial University of Newfoundland, Canada, in 2012, to research subsea flexible pipelines. His experience and research interests include offshore pipelines and floating and fixed platforms, structural integrity, finite element method, fluid structure interaction and offshore structures.

Madjid Abbaspour received an MS degree from MIT, in 1975, and a PhD degree from Cornell University in 1981. He is currently serving as full Professor in the School of Mechanical Engineering at Sharif University of Technology, Tehran, Iran, and head of the Marine Engineering Group. He has more than thirty years working experience in academic areas and in industry. He has published thirteen books in the fields of energy, the environment, and marine engineering.

Rasoul Mohammadi Nasiri received his BS and MS (Artificial Intelligence, 2010) degrees in Computer Engineering from the Computer Engineering Department of Sharif University of Technology, Tehran, Iran. During this time, he worked on computer vision and artificial intelligence, and has taught various courses in computer engineering, including data structures, multimedia systems, and soft computing.